Non-invasive in vitro and in vivo monitoring of degradation of fluorescently labeled hyaluronan hydrogels for tissue engineering applications

Yu Zhang [a,1], Filippo Rossi [b,1,*], Simonetta Papa [c], Martina Bruna Violatto [d], Paolo Bigini [d], Marco Sorbona [a], Francesca Redaelli [a], Pietro Veglianese [c], Jöns Hilborn [a], Dmitri A. Ossipov [a,*]

[a] Science for Life Laboratory, Division of Polymer Chemistry, Department of Chemistry-Ångström, Uppsala University, SE 751 21 Uppsala, Sweden
[b] Department of Chemistry, Materials and Chemical Engineering ''Giulio Natta", Politecnico di Milano, Via Mancinelli, 20131 Milano, Italy
[c] Department of Neuroscience, IRCCS Istituto di Ricerche Farmacologiche Mario Negri, via La Masa 19, 20156 Milano, Italy
[d] Department of Biochemistry and Molecular Pharmacology, IRCCS Istituto di Ricerche Farmacologiche Mario Negri, via La Masa 19, 20156 Milano, Italy

Tracking of degradation of hydrogels-based biomaterials *in vivo* is very important for rational design of tissue engineering scaffolds that act as delivery carriers for bioactive factors. During the process of tissue development, an ideal scaffold should remodel at a rate matching with scaffold degradation. To reduce amount of animals sacrificed, non-invasive *in vivo* imaging of biomaterials is required which relies on using of biocompatible and *in situ* gel forming compounds carrying suitable imaging agents. In this study we developed a method of *in situ* fabrication of fluorescently labeled and injectable hyaluronan (HA) hydrogel based on one pot sequential use of Michael addition and thiol-disulfide exchange reactions for the macromolecules labeling and cross-linking respectively. Hydrogels with different content of HA were prepared and their enzymatic degradation was followed *in vitro* and *in vivo* using fluorescence mul-tispectral imaging. First, we confirmed that the absorbance of the matrix-linked near-IR fluorescent IRDye® 800CW agent released due to the matrix enzymatic degradation *in vitro* matched the amount of the degraded hydrogel measured by classical gravimetric method. Secondly, the rate of degradation was inversely proportional to the hydrogel concentration and this structure–degradation relationship was similar for both *in vitro* and *in vivo* studies. It implies that the degradation of this disulfide cross-linked hyaluronan hydrogel *in vivo* can be predicted basing on the results of its *in vitro* degradation studies. The compliance of *in vitro* and *in vivo* methods is also promising for the future development of predictive *in vitro* tissue engineering models.

Statement of significance

The need for engineered hydrogel scaffolds that deliver bioactive factors to endogenous progenitor cells *in vivo* via gradual matrix resorption and thus facilitate tissue regeneration is increasing with the aging population. Importantly, scaffold should degrade at a modest rate that will not be too fast to support tis-sue growth nor too slow to provide space for tissue development. The present work is devoted to longi-tudinal tracking of a hydrogel material *in vivo* from the time of its implantation to the time of complete resorption without sacrificing animals. The method demonstrates correlation of resorption rates *in vivo* and *in vitro* for hydrogels with varied structural parameters. It opens the possibility to develop predictive *in vitro* models for tissue engineered scaffolds and reduce animal studies.

Keywords: Hyaluronan, Hydrogel degradation, Non-invasive imaging, Spinal cord, Tissue engineering

1. Introduction

During the past decades, extracellular matrix (ECM) mimicking hydrogels have attracted increasing attention in drug delivery and tissue engineering (TE) due to their tissue-resembling properties and the ability to engineer smart responsiveness to external signals

Article history:
Received 19 August 2015
Received in revised form 4 November 2015
Accepted 23 November 2015
Available online 24 November 2015

* Corresponding authors at: Lägerhyddsvägen 1, Box 538, 751 21 Uppsala, Sweden (D.A. Ossipov). Politecnico di Milano, Via Mancinelli, 7, 20131 Milano, (MI), Italy (F. Rossi).
E-mail addresses: filippo.rossi@polimi.it (F. Rossi), dmitri.ossipov@kemi.uu.se (D.A. Ossipov).
[1] These authors contributed equally to this work.

and specific *in vivo* environment [1,2]. Many encouraging results were obtained with different hydrogel-based scaffolds for engineering of de novo tissues. However, very few studies were devoted to unraveling the influence of structural and functional parameters of biomaterials on final tissue engineering effects [3]. Quantitative correlation between tissues formed and the ability of scaffolds to resorb with synchronized rates with respect to new tissue formation is one of the important longitudinal studies that may facilitate rational design of TE scaffolds [4]. Such rational design should first of all rely on suitable *in vitro* degradation models that have fewer and more easily controlled parameters as compared to more complex *in vivo* microenvironment [5]. Additionally, *in vitro* models can study cell-material interactions underlying tissue regeneration processes through the techniques of patterning of various matrix cues on surface [6] or in the bulk [7] of biomaterial. Such studies enable to decouple effects of numerous factors and unambiguously elucidate the role of each factor. Compliance of *in vivo* studies results with the corresponding *in vitro* ones performed on hydrogels with wide ranges of structural parameters should lead to the emergence of *in vitro* TE models with reliable *in vivo* predictability. These models are particularly useful in reduction of animal experiments that are usually required for the assessment of TE capacity of biomaterials. On the other hand, to establish predictive relationships between structural/functional parameters of a hydrogel matrix and its potential to regenerate some particular tissue, initial *in vivo* studies are unavoidable. Longitudinal *in vivo* studies should be therefore based on new non-invasive imaging techniques in order to quantitatively analyze biomaterials *in vivo* without sacrificing large number of animals.

Among different properties of hydrogel-based TE scaffolds that are needed to be quantitatively imaged *in vivo* is biodegradability [8]. During the process of tissue development, an ideal scaffold should remodel at a rate matching with scaffold degradation. In this situation, scaffold degrades enzymatically or hydrolytically at a modest rate that will not be too fast to support tissue growth nor too slow to provide space for tissue development [9]. To date, majority of studies have been limited to monitoring of biomaterials degradation *in vivo* via sampling of explants and analyzing them gravimetrically [10,11] or by another instrumental tools such as gel permeation chromatography (CPG) [12] or fluorescent microscopy [13]. It should be noted that these studies were not truly longitudinal because animals were sacrificed at predetermined time points and could not be followed afterward. Moreover, they were characterized by excessive variability [11,13]. Monitoring of changes in scaffold composition non-invasively over time is a relatively young and unexplored area of research that can overcome the above limitations. Non-destructive techniques employed so far included micro-computed tomography (μ-CT) [14], ultrasound elasticity imaging (UEI) [15], magnetic resonance imaging (MRI) [3,16], and fluorescence multispectral imaging [3–5,17–21]. Particularly, tagging of biomaterials with near-IR fluorescent agents has a potential to eliminate auto-fluorescence from the body and thus increase accuracy of imaging data. However only in few pioneering works utilizing non-invasive fluorescence imaging [4,5], comparative correlation of *in vitro* and *in vivo* degradation data were undertaken for hydrogel materials of similar chemical composition but differing by other parameters influencing the degradation behavior. The importance of such data for the development of predictive *in vitro* TE models is evident.

Hyaluronan (HA) is a natural polysaccharide component of native extracellular matrix, particularly found in high quantities in connective tissues and vitreous of eye. HA is the only non-sulfated glycosaminoglycan of ECM and it plays an important role in regulation of cell–cell interactions, cell-matrix adhesion and cell activation in morphogenesis in human body [22]. Basing on its biocompatibility, native HA was used in treatment of cartilage disease, while cross-linked HA in the form of hydrogels was widely studied for regeneration of bone and artificial aortic heart valves. In TE applications, HA-based hydrogels were acting either as carriers for growth factors or scaffolds for cells [23,24]. Among cancer targeting strategies, HA was utilized in preparation of nanomedicines that can specifically interact with cell surface bound receptor CD44 [25–27]. Nanocomplexes of siRNA with cationic ligand-functionalized HA were also prepared to enter specifically tumor cells overexpressing CD44 receptor and treat them via RNA interference mechanism [28]. A promising field of application for HA hydrogels as scaffold and/or pharmacological delivery tool is spinal cord injury (SCI) [29,30]. SCI is the result of a mechanical damage to the spinal cord that is followed by the "secondary injury, a multifactorial deleterious process that causes most of the post traumatic tissue degeneration. Recent research has focused its attention on multifunctional therapies to counteract the spreading of secondary injury, combining both neuroprotective and neuroregenerative agents. In this field the use of smart hydrogel-based drug delivery systems could provide local multiple drug administration, reducing systemic side effects of drugs and synergizing treatment efficacy [31,32]. As for many other diseases, the fate of these biomaterials within the tissue is uncertain and should be deeply investigated [33].

In this study we report on a strategy that allows tracking of degradation of HA hydrogel-based scaffold *in vivo* employing a non-invasive fluorescence imaging system. This system is based on preparation of two HA derivatives functionalized with mutually reactive chemoselective groups thus permitting formation of a potentially injectable hydrogel *in situ* by simple mixing of aqueous solutions of these derivatives. Due to "click" character of the cross-linking reaction, it can be easily combined *in situ* with labeling of the forming hydrogel with a fluorescent tag bearing suitable chemoselective group. Fluorescently labeled hydrogels with different biopolymer concentration were prepared and the relationship between HA hydrogel mechanical properties and their degradation behavior was investigated. Fluorescence spectroscopy was applied to monitor labeled hydrogel degradation products in real time *in vitro*. Correlations between mechanical properties and hydrogel degradation rate *in vivo* and *in vitro* were established. The hydrogel degradation *in vivo* could be predicted by its degradability *in vitro* thus providing an *in vitro* model system with the potential to avoid extensive animal studies. This strategy can also be expanded to other synthetic and natural polymers as well as to HA derivatives that are dually modified with both cross-linkable groups (such as thiol in this study) and other ligands (cell adhesive peptides, affinity ligands for growth factors, etc.) [34], in order to study the effect of these ligands on hydrogel degradation and tissue regeneration processes. Additionally, the presented HA hydrogel scaffold may be combined with orthogonally labeled drug or growth factor to monitor its release along with the hydrogel degradation and regeneration processes, which makes this approach general.

2. Materials and methods

2.1. Materials

Hyaluronic acid (HA) sodium salt (MW 150 kDa) was purchased from Lifecore Biomedical; *N*-hydroxybenzotriazole (HOBt), 1-ethyl-3-(3-dimethylaminopropyl) carbodiimide (EDC) and DL-dithiothreitol (DTT) were purchased from Sigma–Aldrich Chemical Co. IRDye® 800CW maleimide was purchased from LI-COR Biosciences, Ltd. All solvents were of analytical quality.

2.2. Syntheses of thiol-modified hyaluronic acid (HA-SH)

HA-SH was obtained via carbodiimide mediated coupling between free hydrazide groups of dimeric linker

3′-dithiobispropionic hydrazide (DTP) and carboxylate groups of hyaluronic acid and subsequent *in situ* treatment of the reaction mixture with DTT. Specifically, HA (200 mg, 0.5 mmol of disaccharide repeating units) was dissolved in 25 mL of distilled water and 17.9 mg of DTP (0.075 M equivalents per HA disaccharide unit) was added to HA solution. HOBt (molar ratio to HA disaccharide repeating units as one to one) was separately dissolved in a 1:1 (v/v) mixture of acetonitrile–water at concentration 0.2 M and added to the HA solution. The pH of the resultant solution was adjusted to 4.7 with 1 M NaOH solution. Reaction was initiated by addition of EDC (23.3 mg, 0.15 mmol) to the mixture. After overnight reaction at room temperature, pH of the reaction solution was increased to 8.5 with 1 M NaOH, and 5 M equivalents of DTT (17.9 mg) per HA disaccharide unit was added to the mixture. Reaction continued overnight at room temperature, after which the pH of the mixture was decreased to 3.5 with 1 M HCl solution. The mixture was purified by dialysis in membrane tubes with MW cut off 3,500 Da (Spectra/®Por6, VWR International) against 0.1 M NaCl acidified with hydrochloric acid to pH 3.5 for 18 h once, followed by dialysis against acidified water (pH 3.5) for 18 h two times.

After dialysis, solution was lyophilized to give thiolated HA-SH. The amount of HA-SH product was 156.6 mg (78.3% yield). It was stored at −20 °C. 5 mg of the product was dissolved in 0.6 mL of D_2O to obtain ^1H NMR spectrum on a JEOL JNM-ECP series FT NMR spectrometer (400 MHz). Degree of HA functionalization with thiol groups was determined by comparative integration of ^1H NMR peaks at 2.54 and 2.70 ppm corresponding to the methylene protons of the –C(O)C***H*****$_2$**C***H*****$_2$**SH side chains and a singlet peak at 1.84 ppm corresponding to the acetamide moiety of the *N*-acetyl-D-glucosamine monosaccharide. The degree of HA functionalization with thiol groups was 7.5%.

2.3. Synthesis of 2-dithiopyridyl modified hyaluronic acid (HA-SSPy)

2-Dithiopyridyl functionalized HA (HA-SSPy) was obtained via carbodiimide reaction between 2-(2-pyridinyldithio) ethyl hydrazinecarboxylate (PEH) and hyaluronic acid (HA) sodium salt. In details, HA (300 mg, 0.75 mmol of disaccharide repeating units) was dissolved in 37.5 mL of distilled water, followed by addition of 22 mg (0.12 mmol) of PEH dissolved in 1.8 mL of methanol. HOBt (molar ratio to HA disaccharide repeating units as one to one) was separately dissolved in a 1:1 (v/v) mixture of acetonitrile–water at concentration 0.2 M and added to the HA solution. The pH of the resultant solution was adjusted to 4.7 with 1 M NaOH solution. Reaction was initiated by addition of EDC (21.6 mg, 0.15 mmol) to the mixture. After overnight reaction at room temperature, the mixture was purified by dialysis in membrane tubes with MW cut off 3,500 Da (Spectra/®Por6, VWR International) against 0.1 M NaCl acidified with hydrochloric acid to pH 3.5 for 18 h once, followed by dialysis against acidified water (pH 3.5) for 18 h two times.

After dialysis, the solution was lyophilized to give 279.4 mg (93.1% yield) of 2-dithiopyridyl functionalized HA (HA-SSPy). The obtained product was stored at -20 °C. 5 mg of the product was dissolved in 0.6 mL of D_2O to obtain ^1H NMR spectrum and determine degree of HA functionalization with 2-dithiopyridyl groups. ^1H NMR peaks at 2.70 and 2.89 ppm corresponding to the methylene protons of the –C(O)OC***H*****$_2$C*H*****$_2$**-SS– side chains and peaks at 7.39, 7.63, 7,18 and 8.25 ppm corresponding to four aromatic protons of 2-pyridyl substituent were compared with a singlet peak at 1.84 ppm corresponding to the acetamide moiety of the *N*-acetyl-D-glucosamine residue. Comparison of integrals of the peaks indicated that 5.5% of HA disaccharide monomer units were modified with 2-dithiopyridyl groups.

2.4. In situ preparation of fluorescently labeled HA hydrogels with different polymer concentration

In order to visualize the degradation of HA hydrogel, HA-SH was labeled with a fluorescent dye, IRDye® 800CW maleimide, which is characterized by maximum absorbance wavelength of 774 nm in water. Maleimide group of the dye allows its conjugation to molecules containing free sulfhydryl (–SH) groups through Michael addition reaction. The preparation of labeled hydrogel was realized *in situ* in two steps. The first step comprised of fluorescent labeling of HA-SH using a small fraction of thiol groups for the Michael addition reaction. The second step was the disulfide cross-linking of the labeled HA-SH derivative *in situ* by addition of HA-SSPy derivative. In details, 1.5 mg of HA-SH was dissolved in 150 μL of 10 mM PBS and the obtained solution was neutralized with 7 μL of 0.5 M NaOH solution. The neutralized HA-SH solution was then transferred into an Eppendorf tube containing 20 μg of IRDye® 800CW maleimide (16.7×10^{-3} μmol, i.e. 0.06 M equivalents per thiol group) which initiated Michael addition reaction. After 30 min of the reaction, 150 μL of solution of HA-SSPy in PBS (1%, w/v) was added to the labeled HA-SH solution and the combined solution was vortexed for 3 s. It was then quickly transferred into a head-cut-off syringe mold where disulfide cross-linking proceeded to completion overnight. The hydrogels with 1% concentration was thus formed and were removed from the syringe molds.

Group of hydrogels with 2% concentration was prepared analogously (3 mg of HA-SH in 150 μL of PBS and 3 mg of HA-SSPy in 150 μL of PBS were mixed in this case for preparation of each 2% hydrogel of 300 μL volume). The amount of fluorescent dye was the same for each gel preparation to ensure that hydrogels have the same imaging capacity.

2.5. Study of mechanical properties of hydrogels

After preparation, masses of hydrogels were measured and the hydrogels were transferred into capped glass vials. Mechanical properties of the as prepared hydrogels were studied by rheology using an AR2000 rheometer (TA instruments, Inc., U. K.) with aluminum geometry of 8 mm diameter.

The measurements were taken in the dynamic oscillatory mode at 25 °C with a constant strain of 1% and frequency sweep ranging from 0.1 Hz to 10 Hz.

The hydrogels were washed with 3 mL of PBS for 1 h. This procedure was repeated three times with fresh PBS to ensure that no free (non-covalently linked) fluorescent dye is present in the gels. All hydrogels were finally soaked in 3 mL of PBS overnight to achieve equilibrated swelling state. All medium after washing and swelling was collected to measure the concentration of non-covalently linked fluorescent dye by UV–vis spectrometry and estimate the efficiency of the labeling reaction.

Mechanical properties of the swollen and purified hydrogels were analogously measured by rheology. Swelling ratio of the hydrogels was calculated basing on hydrogel mass in the swollen state.

2.6. In vitro degradation study of hydrogels with different HA concentration

Hydrogels were incubated in 3 mL of PBS containing hyaluronidase (Hase, Sigma–Aldrich Inc., St Louis, MO, 15 units/gel) at 37 °C for 24 h. The medium was removed and substituted with the fresh one containing Hase. The medium after Hase treatment was collected for UV–vis spectrometry analysis (Lambda 35, PerkinElmer Instruments). This procedure was repeated at predetermined time points until the hydrogel was completely degraded.

2.7. Animals care

Procedures involving animals and their care were conducted in conformity with the institutional guidelines at the IRCCS—Institute for Pharmacological Research "Mario Negri" in compliance with national (Decreto Legge nr.116/92, Gazzetta Ufficiale, supplement 40, February 18, 1992; Circolare nr. 8, Gazzetta Ufficiale, July 14, 1994) and international laws and policies (EEC Council Directive 86/609, OJL 358, 1, Dec. 12, 1987; Guide for the Care and Use of Laboratory Animals, US National Research Council (8th edition) 2011).

2.8. Surgery

C57Bl/6 J mice (Charles River Laboratories International, Inc.) were used for *in vivo* studies. Before surgery, animals received an antibiotic and analgesic treatment, respectively with a subcutaneous injection of Ampicillin (50 mg/kg) and Buprenorphine (0.15 mg/kg). The surgical procedure was carried out in deep anesthesia by intraperitoneal injections of Ketamine Hydrochloride (Imalgene, 100 mg/kg) and Medetomidine Hydrochloride (Domitor, 1 mg/kg).

To induce spinal cord exposure, an incision was made in the skin, T11 and T12 vertebrae were identified and exposed by separation of dorsal and intervertebral muscles. Animals were placed on a Cunningham Spinal Cord Adaptor (Stoelting, Dublin, Ireland) mounted on a stereotaxic frame and laminectomy of T12 vertebra was done to uncover the lumbar spinal cord. After spinal cord compression, hydrogels with different concentration (1% and 2%) were placed on the spinal cord.

After spinal cord compression and gel positioning, dorsal muscles were juxtaposed using absorbable sutures and the skin sutured. After the surgery, the animals were kept on a warm pad for 30 min and then placed in separated cages for recovery.

2.9. Non-invasive in vivo degradation study

In vivo whole body fluorescence imaging was performed on 12 mice distributed in two groups treated with hydrogels with different HA concentration (1% and 2%). These mice were analyzed before gel positioning and immediately after, and then at 1, 3, 5 and 7 days after gel positioning. The analysis was carried out using the Explore Optix System (ART Advanced Research Technologies, Montreal, Canada) equipped with a fixed pulsed laser diode as illumination source. Before imaging, animals were anesthetized with a continuous flow of 5% isoflurane, 30% O_2 and 65% NO_2 mixture and placed on their back on a heated (37 °C) pad inside the camera box. Anesthesia (2% isoflurane, 30% O_2 and 68% NO_2) was maintained for the duration of image acquisition using a nose cone delivery system. For each animal, the region of interest (ROI) of the spinal column was chosen with a step size of 2 mm and a spot size of 1 mm. Excitation was performed with a 780 nm pulsing laser and emission was detected with an 820 nm long pass filter. Subsequently, a photomultiplier tube coupled to a time correlated single photon counting system collects the emitted light, allowing detection of the fluorescent signal.

Light emission was recorded as pseudo-color images. Overlay of gray-scale (body reference photograph) and pseudo-color images allowed localization of fluorescent signal. In addition, during the acquisition, a profilometric scan was performed to obtain animal topography. After 14 days, three animals for each group were sacrificed, and their abdominal organs (liver, spleen and kidneys) were removed and scanned for the *ex vivo* fluorescence imaging. Both *in vivo* and *ex vivo* signals related to the selected ROI were quantified as total photon counts using Optiview software (version 2.02.00; ART Advanced Research Technologies).

2.10. Invasive in vivo degradation study

After 3 and 7 days animals with 1% and 2% hydrogels were anesthetized with Equithesin (1% phenobarbital, 4% chloral hydrate, 30 mL/10 g, i.p.) and transcardially perfused with 20 mL saline and subsequently with 50 mL of sodium phosphate buffered 4% formaldehyde solution. Spinal cords were rapidly removed and the recovered hydrogels were washed with PBS, lyophilized and then weighted to estimate the percentage of degradation.

2.11. Statistical analysis

Where applicable, experimental data were analyzed using Analysis of Variance (ANOVA). Statistical significance was set to p value < 0.05. Results are presented as mean value ± standard deviation.

3. Results and discussions

3.1. Synthesis of thiol and 2-dithiopyridyl functionalized HA derivatives

Previously, hyaluronic acid hydrogels have been prepared by variety of cross-linking methods including chemoselective reactions such as azide-alkyne cycloaddition click reaction [35], aqueous Diels–Alder chemistry [36], peroxidase-catalyzed oxidation of tyramine [37], oxime coupling [38], Michael addition of thiols to vinylsulfone [39] or acrylates [40], and thiol-disulfide exchange reaction [41]. These chemoselective reactions allow *in situ* encapsulation of cells and relevant complex biomacromolecules such as growth factors in hydrogel carriers without affecting their bioactivity as well as they form no toxic side products. We have chosen a thiol-disulfide exchange reaction to cross-link HA chains because it proved to be the most cytocompatible for several different cell types *in vitro* [41]. As compared to previously reported disulfide cross-linking of HA by autoxidation of thiols [42], we sought to accelerate the reaction by applying an activated disulfide component such as 2-dithiopyridyl. We anticipated that this could be achieved by using two HA derivatives functionalized with thiol (HA-SH) and 2-dithiopyridyl groups (HA-SSPy) respectively.

Two known reagents, 3,3′-dithiobispropionic hydrazide (DTP) [43] and 2-(2-pyridinyldithio) ethyl hydrazinecarboxylate (PEH) [44], were utilized for preparation of HA-SH and HA-SSPy derivatives respectively. Carboxylate groups of native HA (Scheme 1) were activated with carbodiimide (EDC) and *N*-hydroxybenzotriazole (HOBt) and then coupled to hydrazide groups of the linkers through amide bonds. Due to the presence of two hydrazide groups in DTP reagent, it could potentially form cross-links between two different HA macromolecules or within the same HA macromolecule (first step in Scheme 1a). However, after one pot treatment of the reaction mixture with a reducing agent dithiothreitol (DTT), the formed cross-links were broken along the disulfide bond leaving the two free thiol groups (second step in Scheme 1a). ^{1}H NMR analysis of the product showed that 7.5% of the disaccharide repeating units of HA were modified with thiol groups (Fig. 1). Synthesis of 2-dithiopyridyl modified HA was completed in one step by carbodiimide-mediated amide coupling of PEH to HA (Scheme 1b). The modification of HA by 2-dithiopyridyl groups was 5.5% according to ^{1}H NMR spectrum (Fig. 2). The functionalization of HA-SH was 7.5%, i.e. higher than 5.5% functionalization of HA-SSPy, leaving the possibility for use of the excess of the thiol groups for attachment of a fluorescent label.

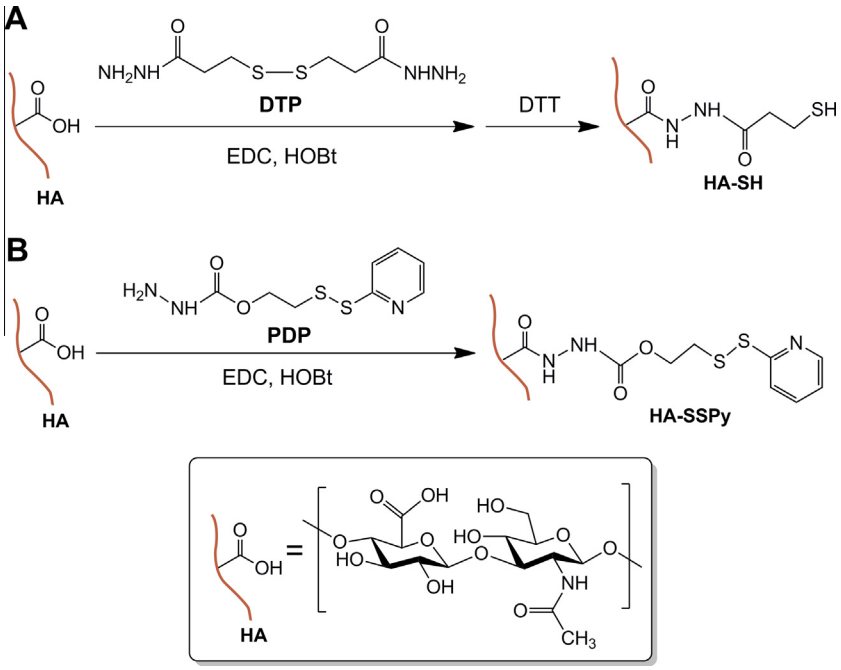

Scheme 1. Functionalization of hyaluronic acid (the structure is shown in the box) with (a) DTP to give HA-SH derivative and (b) with PDP to give HA-SSPy derivative.

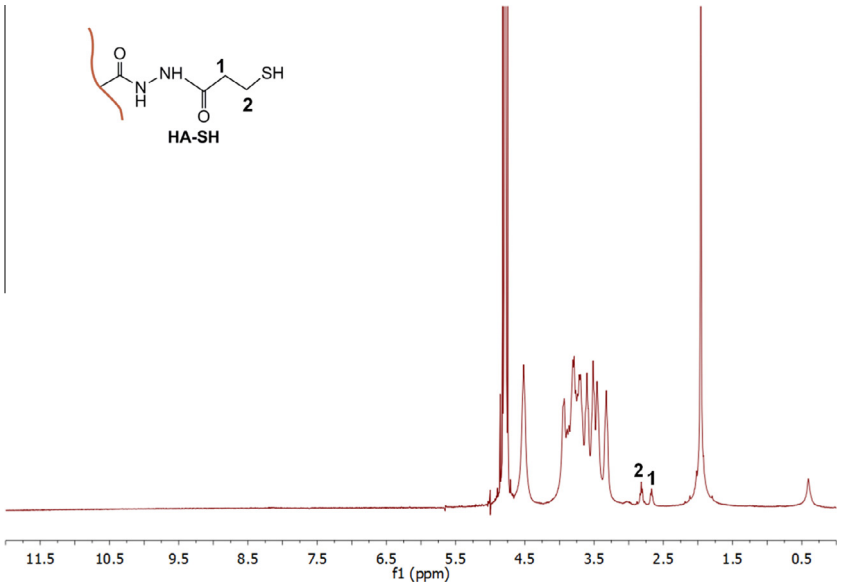

Fig. 1. ^{1}H NMR spectrum of thiol-derivatized HA (HA-SH).

3.2. Preparation of IRDye® 800CW labeled HA hydrogel

First, we confirmed that mixing of aqueous solutions of HA-SH and HA-SSPy derivatives permitted quick sol-to-gel transformation as compared with the previously reported cross-linking of HA by homo-bifunctional PEG cross-linker [41]. As expected, the rate of thiol-disulfide exchange reaction was dependent on pH affording hydrogels in less than 30 s at pH 7.4. By lowering pH, the time for reaching of sol–gel transition could be extended to several minutes.

Thiol group in HA-SH derivative can also be tagged with a labeling agent bearing suitable reactive groups such as acrylate, vinylsufone, maleimide or 2-dithiopyridyl. Importantly, this labeling reaction can be performed *in situ*, i.e. without isolation of the intermediated product but instead by directly proceeding with the cross-linking of the labeled HA-SH derivative. Particularly, in this work we employed Michael addition of thiol groups of HA-SH to double bond of maleimide group of IRDye® 800CW fluorescent dye via a thioether linkage. Scheme 2 shows *in situ* preparation of fluorescently labeled HA hydrogel through sequential Michael addition conjugation reaction and disulfide cross-linking reaction. To ensure that thiol groups are deprotonated and generate nucleophilic species, Michael addiction reaction to maleimide group was performed at pH 7.5 for 30 min after which, solution of HA-SSPy was added to the mixture. The remaining thiol groups of HA-SH in the form of thiolate anions (RS^{-}) displaced 2-thiopyridine in the course of S_N2 nucleophilic substitution reaction and formed disulfide cross-linkages. It should be noted that only

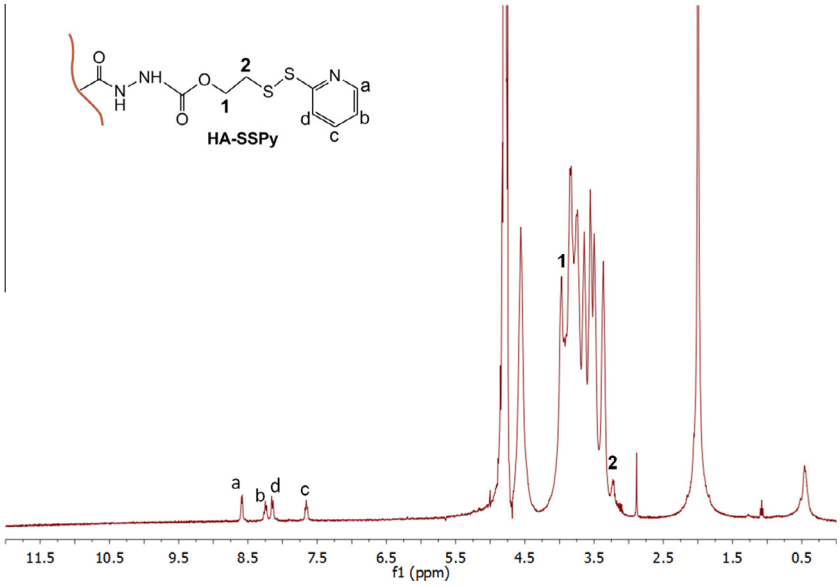

Fig. 2. ^{1}H NMR spectrum of 2-dithiopyridyl-derivatized HA (HA-SSPy).

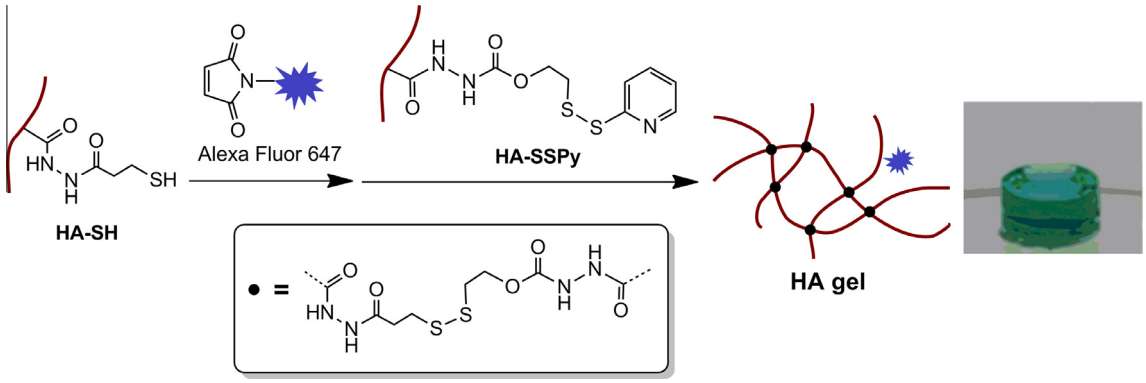

Scheme 2. *In situ* fabrication of fluorescently labeled HA hydrogel.

tiny fraction of thiol groups was anticipated to react with fluorescent labeling agent in order to minimize the effect of the agent on the decrease of hydrogel cross-linking density. On the other hand, preparation of the hydrogel at physiological pH provided an opportunity of direct administration of the hydrogel *in vivo* through the injection.

It was important to ensure that fluorescent tag was covalently linked to the resulting matrix in order to accurately confront the fluorescence of the liquid degradation medium with the hydrogel degradation. Only by eliminating any physically trapped fluorescent species from a hydrogel material, one can quantitatively assess the degradation process of the hydrogel *in vitro* by measuring the fluorescence of the hydrogel degradation products released from the hydrogel into the liquid phase. Therefore, the hydrogels after setting were repeatedly swollen in fresh PBS for several times and the liquid phases were collected for UV–vis spectroscopic analysis. It appeared that *in situ* labeling reaction occurred with nearly 75% yield and the rest of the labeling agent was released from the hydrogel during the first three rounds of the hydrogel swelling (Fig. S1 in Supporting information). No detectable by UV–vis spectrometry species from the fluorescent label were observed in further liquid media indicating that the hydrogel contained only covalently linked label after this purification procedure.

3.3. Study of mechanical properties of hydrogels

Stiffness and elasticity of hydrogels have an important impact in biomedical application. Ideally, mechanical properties of a hydrogel should match the stiffness of a tissue to be regenerated. These properties can be controlled through varying cross-linking density of hydrogels, which depend in turn either on degree of functionalization of macromolecular precursors with the functional groups undergoing cross-linking or concentration of the precursors. In order to investigate the influence of HA concentration on hydrogel stiffness and subsequently on its degradation, we have prepared two types of hydrogels with 1% and 2% of HA content. It proved that stiffness of a hydrogel was correlated with its cross-linking density. We observed that hydrogel with 2% concentration had a 2.2-fold higher storage modulus than a hydrogel with 1% concentration before swelling (Table 1). After hydrogel swelling, this difference further increased and reached a value of 2.5-fold.

3.4. In vitro study of hydrogel degradation

Taking into account that only 75% of the fluorescent label was covalently linked after *in situ* labeling reaction, all hydrogels were washed four times in PBS before they were subjected to *in vitro* or

Table 1
Storage modulus (G′) of hydrogels with different cross-linking density before and after swelling in PBS.

Hydrogel	G′ before swelling (Pa)	G′ after swelling (Pa)	Swelling ratio*
1% HA	752.6 ± 16.1	731.88 ± 14.0	44.8 ± 1.5
2% HA	1649.8 ± 230.9	1832.3 ± 179.8	51.4 ± 2.8

* Swelling ratio = weight of a swollen sample/dry weight of the sample.

in vivo degradation studies. The medium after washings was collected and measured by UV–vis spectrometry in order to confirm that the all washed hydrogels did not contain free fluorescent agent. Enzymatic degradation of the hydrogels was subsequently performed by placing the hydrogels into solution of hyaluronidase in PBS. The enzyme solution was changed daily into a fresh one. It was assumed that as the hydrogels degraded, fluorescently labeled HA fragments were released from the hydrogels. By measuring fluorescence intensity of the liquid samples we were able to calculate the amount of HA that was released and compared it with the total one used for the hydrogel formation.

Hydrogels degradation was followed for 6 days and it was observed that hydrogel with 1% concentration (marked as *Hydrogel-1*) degraded completely in four days (Fig. 3a). On the other hand, hydrogel with 2% concentration (marked as *Hydrogel-2*) degraded in six days. These results were as expected, *i.e.* more stiffer hydrogel with higher concentration lasted longer upon enzymatic degradation *in vitro*. As it can be seen from Fig. 3a, *Hydrogel-1* released the highest amount of fluorescent HA degradation products on the second day of the degradation study. After two days, the amount of degraded products started to decline due to the fact that most of the hydrogel had been already degraded. Contrary, *Hydrogel-2* showed a more sustained degradation during the whole period of six days. Degradation of 2% hydrogel reached its maximum also on the second day and the rate of degradation remained the same during the next three days. Only on the last sixth day, the degradation was diminished because of the little amount of the hydrogel remained at this time point. These results can be explained by the necessity for the diffusion of hyaluronidase from the liquid phase into the hydrogel network. Most probably, at the start of the degradation experiment, the diffusion of the enzyme into a denser network is limited and degradation of *Hydrogel-2* occurs mainly by erosion (*i.e.* from the surface). Contrary, more facile diffusion of Hase into *Hydrogel-1* resulted in the fast bulk degradation.

Cumulative absorbance of the released fluorescent HA degradation products were plotted and related to the whole amount of fluorescent HA material used for hydrogel preparation. It allowed calculation of the percentage of the hydrogels degraded over the time (Fig. 3b). Thus, it was clearly demonstrated that *Hydrogel-1* had a faster rate of degradation compared to *Hydrogel-2*. Specifically, more than 50% of *Hydrogel-1* degraded during the first two days. Contrary, *Hydrogel-2* showed a degradation profile with lower slope over six days. In order to validate that monitoring of hydrogel degradation by measuring UV–vis absorbance of the degraded products is acceptable, we have compared it with the monitoring of hydrogels mass loss during the degradation. For that, the collected supernatants for each time point were first desalted by dialysis and then freeze-dried to get the mass of degradation products. Fig. 4 shows the cumulative percentage of hydrogel mass that was degraded over the time of enzymatic degradation study. As we expected, the rate of degradation of 1% hydrogel was higher than the degradation rate for 2% hydrogel. Thus, the same degradation trend was observed when measuring the loss of hydrogel mass. Essentially, using the gravimetric analysis for degradation, we could confirm that more than 50% of *Hydrogel-1* was degraded during the first two days, whereas *Hydrogel-2* was degraded with slower rate over 6 days (Fig. 4).

Finally, we correlated the degradation curves for both *Hydrogel-1* and *Hydrogel-2* determined by two methods, i.e. by measuring the hydrogel mass and measuring UV–vis absorbance of the degradation products in the liquid phase (Fig. S2). The curves for hydrogel mass loss and UV–vis absorbance of degradation products coincided for two types of hydrogels. It demonstrated that hydrogel degradation can be quantified *in vitro* through measuring the fluorescence intensity.

3.5. Non-invasive and invasive in vivo hydrogel degradation

To investigate the effect of hyaluronidase-mediated local biodegradation in the body, IRDye® 800CW-labeled HA hydrogel scaffolds were implanted into the spinal cord of mice. Mice injected with *Hydrogel-1* and *Hydrogel-2* were analyzed qualitatively and quantitatively by measuring relative fluorescence intensity with respect to the time of implantation. It is known that

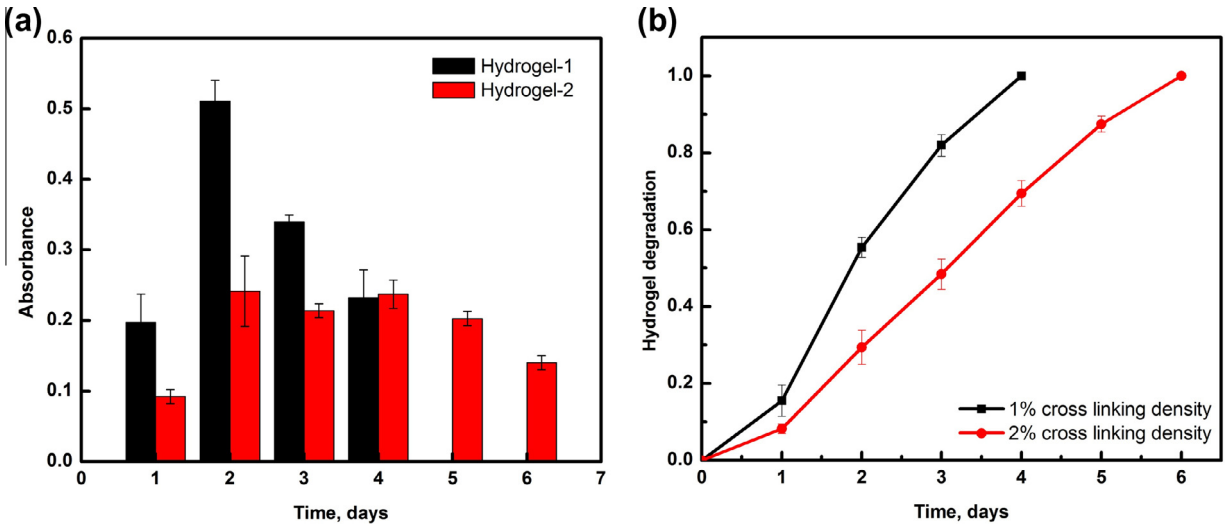

Fig. 3. (a) UV–vis absorbance of medium obtained after degradation of hydrogels at different time intervals. Absorbance at 789 nm was measured. (b) Cumulative degradation profiles of *Hydrogel-1* (black curve) and *Hydrogel-2* (red curve). (For interpretation of the references to color in this figure legend, the reader is referred to the web version of this article.)

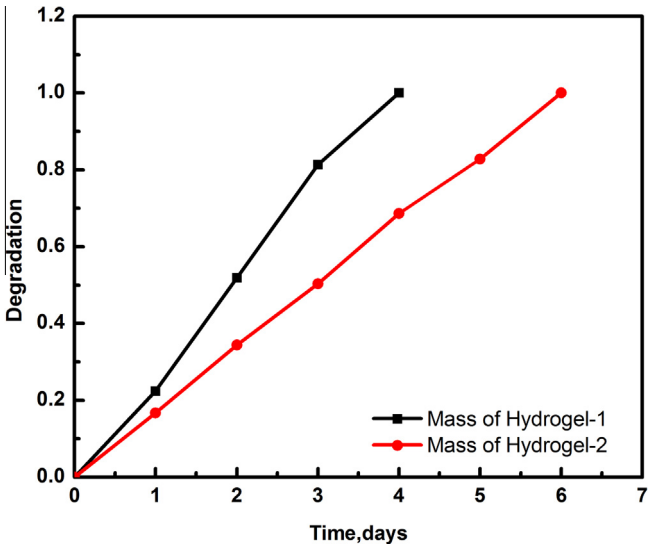

Fig. 4. Degradation profiles for *Hydrogel-1* (black curve) and *Hydrogel-2* (red curve) determined by measuring the hydrogels mass loss. (For interpretation of the references to color in this figure legend, the reader is referred to the web version of this article.)

mechanical stress around the implanted scaffold is a key determining factor for the degree of reaction of organism to the foreign body, which stimulates collagenase production and release of growth factors from fibroblasts, macrophages and neutrophils [45,46].

As shown in Fig. 5a and b, a significant decrease in the fluorescence signal was observed from the scaffold over the time after implantation. Because IRDye® 800CW-labeled HA hydrogels are stable in buffer solution, the signal reduction in the body should arise from enzymatic degradation of HA hydrogel, release and diffusion of biodegraded HA fragments away from the site of implantation. Qualitative comparison of images obtained from animals implanted with *Hydrogel-1* with *Hydrogel-2* indicated that *Hydrogel-1* (Fig. 5a) degraded in less than 3 days, while degradation of *Hydrogel-2* took longer time (Fig. 5b). Measurement of relative intensity over time could give a reliable quantitative assessment of scaffold degradation and the loss of fluorescence signal with time *in vivo* was converted into the weight loss over the time as shown in Fig. 6. Thus, it was clearly demonstrated that *Hydrogel-1* showed a faster rate of degradation compared to *Hydrogel-2*. Specifically, *Hydrogel-1* degraded completely at day 3 after implantation. Contrary, 50% of *Hydrogel-2* was still left *in vivo* at this time and degradation was gradually continued over last three days. It should be noted, however, that in contrast to *in vitro* degradation in PBS buffer, both hydrogels with different cross-linking densities were characterized by substantial degradation during the first day *in vivo*. This observed difference in degradation reflects different environmental factors that affect the hydrogel resorption *in vitro* and *in vivo*. Apart from the day 1, the *in vivo* results demonstrated a good correlation with the *in vitro* degradation profiles shown in Fig. 4.

In order to confirm that non-invasive monitoring of the fluorescence signal indeed reflected real mass loss for the implanted hydrogel due to its enzymatic resorption, we performed a parallel *in vivo* scaffold degradation study by classic invasive sampling of hydrogels explants followed by gravimetric determination. Three mice implanted with *Hydrogel-1* and three mice implanted with *Hydrogel-2* were sacrificed after 3 and 7 days of implantation and the remaining scaffolds was recovered (see the details in Fig. S3), washed, lyophilized and finally weighted. The results were plotted as percentage of the resorbed hydrogel versus time and correlated with the analogous results obtained from the non-invasive studies

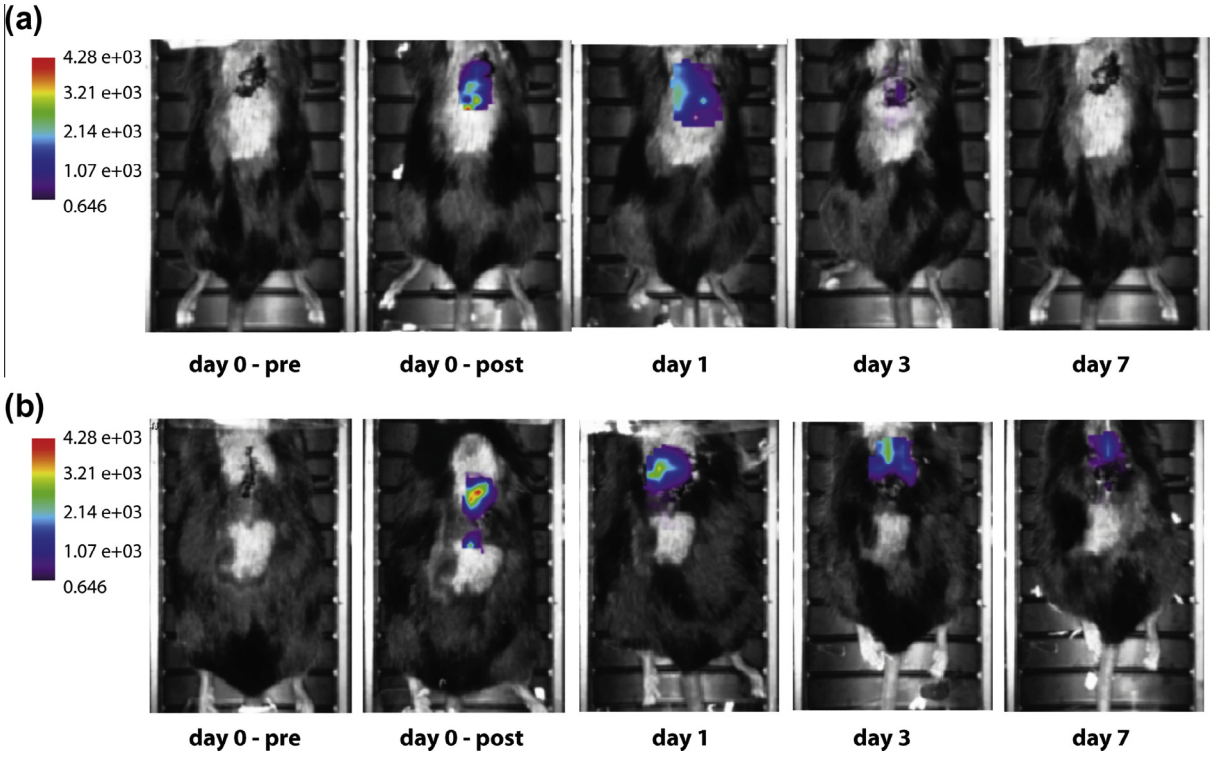

Fig. 5. *In vivo* non-invasive representative images from longitudinal study of scaffold degradation as a function of hydrogel concentration: (a) *Hydrogel-1*, (b) *Hydrogel-2*. Different time points were evaluated: pre-positioning, post-positioning ($t = 0$), 1 day, 2 days, 3 days and 7 days after gel positioning. At $t = 0$ the fluorescence signal was localized in a clearly defined space corresponding to the gel. A progressive reduction of fluorescence intensity was observed in both hydrogels but with different rates.

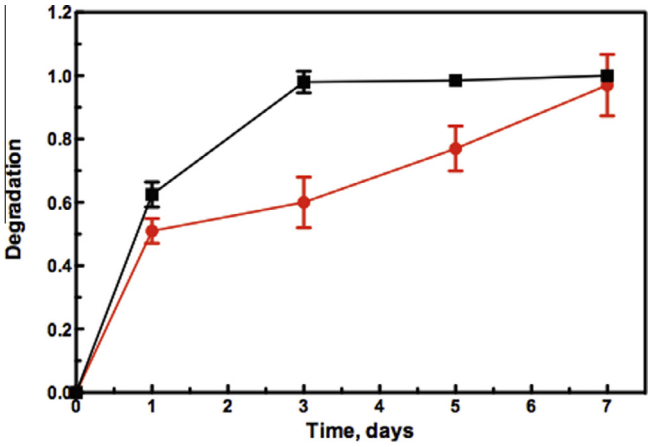

Fig. 6. The course of weight loss for labeled hydrogels over the time *in vivo*. Black curve corresponds to *Hydrogel-1* with 1% concentration and red curve corresponds to *Hydrogel-2* with 2% concentration. The weight loss was derived from the loss of fluorescence signal intensity.

(Fig. 7). It was noteworthy that values for hydrogel mass loss obtained from non-invasive studies coincided with respective values obtained from invasive studies for both types of hydrogels and both time points taken at the middle and at the end of the studies. This comparison underlined the suitability of non-invasive fluorescence imaging methods to follow scaffold degradation *in vivo*.

3.6. In vivo biodistribution and clearance

To determine the biodistribution and clearance of products of the HA hydrogels degradation, animals were sacrificed after 14 days of implantation and *ex vivo* optical scanning was carried out for isolated liver, kidney, spleen, and lung, *i.e.* for the filter organs. This evaluation demonstrated that degradation products from the IRDye® 800CW-labeled HA hydrogel scaffolds were not significantly present in these organs (Fig. 8). The observed fluorescence of the organs after 14 days of hydrogels implantation was very low and typical of auto-fluorescence of tissues. Importantly, the same marginal values of fluorescence were observed for control animals not implanted with hydrogels. More accurate analysis of the explanted organs by mass spectrometry is however still needed to monitor the fate of the IRDye® 800CW-labeled HA degradation products. Basing on fluorescence measurements we assumed that the degradation products could be almost completely removed from the body after 14 days of the hydrogels implantation. The same results were obtained for mice implanted with both *Hydrogel-1* and *Hydrogel-2*. For sake of simplicity we reported here only the results of analysis for *Hydrogel-2* in Fig. 8.

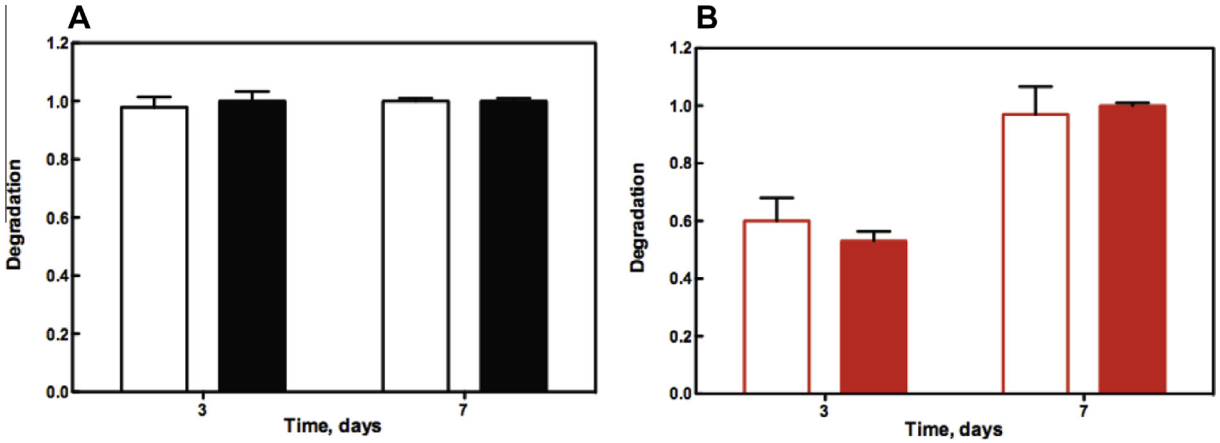

Fig. 7. Correlation of HA hydrogel degradation quantified by applying non-invasive (empty columns) and invasive methods (full-colored columns) for (a) *Hydrogel-1* and (b) *Hydrogel-2*. (For interpretation of the references to color in this figure legend, the reader is referred to the web version of this article.)

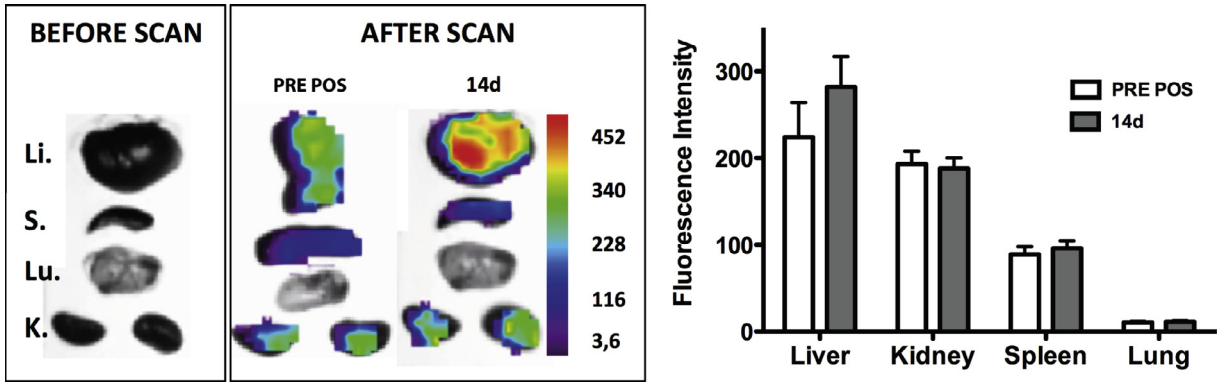

Fig. 8. Bio-distribution and clearance of the degradation products derived from the implanted IRDye® 800CW-labeled HA hydrogel scaffolds. The following abbreviations were used for the studied organs: Li – liver, S – spleen, Lu – lung, K – kidney. Fluorescence scan images were taken at the time of pre-positioning ($t = 0$) and after 14 days of implantation. Quantification of the fluorescence intensity revealed comparable values for pre-positioning (PRE POS) and after-degradation (14 days) animals.

4. Conclusion

Tracking of degradation of hydrogels-based biomaterials *in vivo* is very important for rational design of tissue engineering scaffolds that act as delivery carriers for bioactive factors. However, in order to establish relationships between the amount and quality of tissue formed and the mode of release determined by degradation of a bulk hydrogel-based material, extensive animal studies have to be performed. Reduction of number of sacrificed animals can be achieved by using methods of non-invasive *in vivo* imaging of biomaterials. In this study we developed an *in situ* method of fabrication of fluorescently labeled potentially injectable hydrogel that can be imaged *in vivo* throughout the whole time period of a longitudinal study. This method is based on one pot sequential use of Michael addition reaction and thiol-disulfide exchange reaction for macromolecules labeling and cross-linking respectively. Using hyaluronic acid as an example of a biocompatible biopolymer, we demonstrated that around 75% of near-IR fluorescent agent IRDye® 800CW maleimide could be incorporated into HA macromolecule functionalized with thiol groups followed by *in situ* transformation of the liquid mixture into a self-standing hydrogel within a minute. Due to "click" character of the employed reactions, this fabrication method can be easily extended for *in situ* three-dimensional encapsulation of growth factors or/and cells in the hydrogel material. *In vitro* enzymatic degradation studies was followed by UV–vis spectrometry and demonstrated that the rate of HA hydrogels degradation was inversely dependent on the concentration of the hydrogels. This trend was also observed *in vivo* though quantitative monitoring of the decay of fluorescence signal over 7 days of longitudinal studies. Thus, the compliance of *in vitro* and *in vivo* methods is a promising observation that opens a way to establishing of predictive *in vitro* tissue engineering models. This work is a first step in future development of such models through comparative tracking of biomaterials degradation, release and distribution of morphogenetic factors, and new tissues formed. The presented method can be also extended to other types of hydrogels prepared from other biocompatible natural and synthetic macromolecules.

Disclosures

No potential conflicts of interest exist.

Acknowledgements

The research leading to these results has received funding from the European Community's Seventh Frame-work Programme (BIODESIGN). Y. Zhang thanks to scholarship supported by China Scholar Council (CSC).

Appendix A. Figures with essential color discrimination

Certain figures in this article, particularly Figs. 5 and 8, are difficult to interpret in black and white. The full color images can be found in the on-line version.

Appendix B. Supplementary data

Supplementary data associated with this article can be found, in the online version, at http://dx.doi.org/10.1016/j.actbio.2015.11.053.

References

[1] D. Seliktar, Designing cell-compatible hydrogels for biomedical applications, Science 336 (2012) 124–128.
[2] T. Hoare, D. Kohane, Hydrogels in drug delivery: progress and challenges, Polymer 49 (2008) 1993–2007.
[3] A. Berdichevski, H. Yameen, H. Dafni, M. Neeman, D. Seliktar, Using bimodal MRI/fluorescence imaging to identify host angiogenic response to implants, Proc. Natl. Acad. Sci. 112 (2015) 5147–5152.
[4] N. Artzi, N. Oliva, C. Puron, S. Shiteet, S. Artzi, A.B. Ramos, A. Groothuis, G. Sahagian, E. Edelman, In vivo and in vitro tracking of erosion in biodegradable materials using non-invasive fluorescence imaging, Nat. Mater. 10 (2011) 704–709.
[5] W. Wang, J. Liu, C. Li, J. Zhang, J. Liu, A. Dong, D. Kong, Real-time and non-invasive fluorescence tracking of in vivo degradation of the thermosensitive PEGlyated polyester hydrogel, J. Mater. Chem. B 2 (2014) 4185–4192.
[6] X. Yao, R. Peng, J. Ding, Cell-material interactions revealed via material techniques of surface patterning, Adv. Mater. 25 (2013) 5257–5286.
[7] K.A. Mosiewicz, L. Kolb, A.J. van der Vlies, M.M. Martino, P.S. Lienemann, J.A. Hubbell, M. Ehrbar, M.P. Lutolf, In situ cell manipulation through enzymatic hydrogel photopatterning, Nat. Mater. 12 (2013) 1072–1078.
[8] K. Bae, L. Wang, M. Kurisawa, Injectable biodegradable hydrogels: progress and challenges, J. Mater. Chem. B 1 (2013) 5371–5388.
[9] J. Zhu, R.E. Marchant, Design properties of hydrogel tissue-engineering scaffolds, Expert Rev. Med. Devices 8 (2011) 607–626.
[10] C.J. Bettinger, J.P. Bruggeman, J.T. Borenstein, R.S. Langer, Amino alcohol-based degradable poly (ester amide) elastomers, Biomaterials 105 (2008) 2315–2325.
[11] A. Mahdavi, L. Ferreira, C. Sundback, J.W. Nikol, E.P. Chan, D.J.D. Carter, C.J. Bettinger, S. Patanavanich, L. Chignozha, E. Ben-Joseph, A. Galakatos, H. Pryor, I. Pomerantseva, P.T. Masiakos, W. Faquin, A. Zumbuehl, S. Hong, J. Borenstein, J. Vacanti, R. Langer, J.M. Karp, A biodegradable and biocompatible gecko-inspired tissue adhesive, Proc. Natl. Acad. Sci. 105 (2008) 2307–2312.
[12] A.C.R. Grayson, G. Voskerician, A. Lynn, J.M. Anderson, M.J. Cima, R. Langer, Differential degradation rates in vivo and in vitro of biocompatible poly(lactic acid) and poly(glycolic acid) homo- and co-polymers for a polymeric drug-delivery microchip, J. Biomater. Sci. Polym. Ed. 15 (2004) 1281–1304.
[13] O. Benny, S.-K. Kim, K. Gvili, I.S. Radzishevsky, A. Mor, L. Verduzco, L.G. Menon, P.M. Black, M. Machluf, R.S. Carroll, In vivo fate and therapeutic efficacy of PF-4/CTF microspheres in an orthotopic human glioblastoma model, FASEB J. 22 (2008) 488–499.
[14] G. Lenthea, H. Hagenmüller, M. Bohner, S. Hollistere, L. Meinelc, R. Müller, Nondestructive micro-computed tomography for biological imaging and quantification of scaffold-bone interaction in vivo, Biomaterials 28 (2007) 2479–2490.
[15] K. Kim, C.G. Jeong, S.J. Hollister, Non-invasive monitoring of tissue scaffold degradation using ultrasound elasticity imaging, Acta Biomater. 4 (2008) 783–790.
[16] Y. Liang, A. Bar-Shir, X. Song, A.A. Gilad, P. Walczak, J.W.M. Bulte, Label-free imaging of gelatin-containing hydrogel scaffolds, Biomaterials 42 (2015) 144–150.
[17] C. Cunha-Reis, A. El Haj, X. Yang, Y. Yang, Fluorescent labeling of chitosan for use in non-invasive monitoring of degradation in tissue engineering, J. Tissue Eng. Regen. Med. 7 (2013) 39–50.
[18] D.E. Soranno, H.D. Lu, H.M. Weber, R. Rai, J.A. Burdick, Immunotherapy with injectable hydrogels to treat obstructive nephropathy, J. Biomed. Mater. Res. A 102 (2014) 2173–2180.
[19] C.B. Rodell, J.W. MacArthur Jr., S.M. Dorsey, R.J. Wade, L.L. Wang, Y.J. Woo, J.A. Burdick, Shear-thinning supramolecular hydrogels with secondary autonomous covalent crosslinking to modulate viscoelastic properties in vivo, Adv. Funct. Mater. 25 (2015) 636–644.
[20] S.H. Kim, J.H. Lee, H. Hyun, Y. Ashitate, G. Park, K. Robichaud, E. Lunsford, S.J. Lee, G. Khang, H.S. Choi, Near-infrared fluorescence imaging for noninvasive trafficking of scaffold degradation, Sci. Rep. 3 (2013) 1–7.
[21] L. Möller, A. Krause, I. Bartsch, A. Kirschning, F. Witte, G. Dräger, Preparation and in vivo imaging of lucifer yellow tagged hydrogels, Macromol. Symp. 309 (310) (2011) 222–228.
[22] E.J. Menzel, C. Farr, Hyaluronidase and its substrate hyaluronan: biochemistry, biological activities and therapeutic uses, Cancer Lett. 11 (1998) 3–11.
[23] G. Hulsart-Billström, P. Yuen, R. Marsell, J. Hilborn, S. Larsson, D. Ossipov, Bisphosphonate-linked hyaluronic acid hydrogel sequesters and enzymatically releases active bone morphogenetic protein-2 for Induction of osteogenic differentiation, Biomacromolecules 14 (2013) 3055–3063.
[24] C. Chung, J.A. Burdick, Influence of three-dimensional hyaluronic acid microenvironments on mesenchymal stem cell chondrogenesis, J. Tissue Eng. Regen. Med. A 15 (2009) 243–254.
[25] D. Ossipov, S. Kootala, Z. Yi, X. Yang, J. Hilborn, Orthogonal chemoselective assembly of hyaluronic acid networks and nanogels for drug delivery, Macromolecules 46 (2013) 4105–4113.
[26] X. Wei, T.H. Senanayake, G. Warren, S.V. Vinogradov, Hyaluronic acid-based nanogel-drug conjugates with enhanced anticancer activity designed for targeting of CD44-positive and drug-resistant tumors, Bioconjugate Chem. 17 (2013) 658–668.
[27] Y. Zhang, Y. Sun, X. Yang, J. Hilborn, A. Heerschap, D. Ossipov, Injectable in situ forming hybrid iron oxide-hyaluronic acid hydrogel for magnetic resonance imaging and drug delivery, Macromol. Biosci. 14 (2014) 1249–1259.
[28] S. Ganesh, A.K. Iyer, D. Morrissey, M.M. Amiji, Hyaluronic acid based self-assembling nanosystems for CD44 target mediated siRNA delivery to solid tumors, Biomaterials 34 (2013) 3489–3502.
[29] I.E. Donaghue, C.H. Tator, M.S. Shoichet, Hyperbranched PEG-based supramolecular nanoparticles for acid-responsive targeted drug delivery, Biomater. Sci. 3 (2015) 65–72.

[30] R.Y. Tam, T. Fuehrmann, N. Mitrousis, M.S. Shoichet, Regenerative therapies for central nervous system diseases: a biomaterials approach, Neuropsychopharm. Rev. 39 (2014) 169–188.
[31] G. Perale, F. Rossi, M. Santoro, M. Peviani, S. Papa, D. Llupi, P. Torriani, E. Micotti, S. Previdi, L. Cervo, E. Sundström, A.R. Boccaccini, M. Masi, G. Forloni, P. Veglianese, Multiple drug delivery hydrogel system for spinal cord injury repair strategies, J. Control. Release 159 (2012) 271–280.
[32] I. Caron, S. Papa, F. Rossi, G. Forloni, P. Veglianse, Nanovector-mediated drug delivery for spinal cord injury treatment, WIREs Nanomed. Nanobiotechnol. 6 (2014) 506–515.
[33] B. Shrestha, K. Coykendall, Y. Li, A. Moon, P. Priyadarshani, L. Yao, Repair of injured spinal cord using biomaterial scaffolds and stem cells, Stem Cell Res. Ther. 5 (2014) 91–101.
[34] M. Kisiel, M. Martino, M. Ventura, J. Hubbell, J. Hilborn, D.A. Ossipov, Improving the osteogenic potential of BMP-2 with hyaluronic acid hydrogel modified with integrin-specific fibronectin fragment, Biomaterials 34 (2013) 704–712.
[35] A. Takahashi, Y. Suzuki, T. Suhara, K. Omichi, A. Shimizu, K. Hasegawa, N. Kokudo, S. Ohta, T. Ito, In situ cross-linkable hydrogel of hyaluronan produced via copper-free click chemistry, Biomacromolecules 14 (2013) 3581–3588.
[36] H. Tan, P. Rubin, K.G. Marra, Direct synthesis of biodegradable polysaccharide derivative hydrogels through aqueous diels-alder chemistry, Macromol. Rapid Commun. 32 (2011) 905–911.
[37] F. Lee, J.E. Chung, M. Kurisawa, An injectable enzymatically crosslinked hyaluronic acid–tyramine hydrogel system with independent tuning of mechanical strength and gelation rate, Soft Matter 4 (2008) 880–887.
[38] G.N. Grover, R.L. Braden, K.L. Christman, Oxime cross-linked injectable hydrogels for catheter delivery, Adv. Mater. 25 (2013) 2937–2942.
[39] R. Jin, L. Moreira Teixeira, A. Krouwels, P. Dijkstra, C.A. van Blitterswijk, M. Karperien, J. Feijen, Synthesis and characterization of hyaluronic acid-poly (ethylene glycol) hydrogels via Michael addition: an injectable biomaterial for cartilage repair, Acta Biomater. 6 (2010) 1968–1977.
[40] J. Zhang, A. Skardal, G.D. Prestwich, Engineered extracellular matrices with cleavable crosslinkers for cell expansion and easy cell recovery, Biomaterials 29 (2008) 4521–4531.
[41] S.Y. Choh, D. Cross, C. Wang, Facile synthesis and characterization of disulfide-cross-linked hyaluronic acid hydrogels for protein delivery and cell encapsulation, Biomacromolecules 12 (2011) 1126–1136.
[42] X. Shu, Y. Liu, Y. Luo, F. Palumb, G. Prestwich, Disulfide-crosslinked hyaluronan-gelatin hydrogel films: a covalent mimic of the extracellular matrix for in vitro cell growth, Biomaterials 24 (2003) 3825–3834.
[43] X.Z. Shu, Y. Liu, Y. Luo, M.C. Roberts, G.D. Prestwich, Disulfide cross-linked hyaluronan hydrogels, Biomacromolecules 3 (2002) 1304–1311.
[44] T. Kaneko, D. Willner, I. Mankovic, J.O. Knipe, G.R. Braslawsky, R.S. Greenfield, D.M. Vyas, New hydrazone derivatives of Adriamycin and their immunoconjugates – a correlation between acid stability and cytotoxicity, Bioconjugate Chem. 2 (1991) 133–141.
[45] J. Hilborn, L.M. Bjursten, A new and evolving paradigm for biocompatibility, J. Tissue Eng. Regen. Med. 1 (2007) 110–119.
[46] J. Gross, E. Harper, E.D. Harris, P.A. McCroskery Jr., J.H. Highberger, C. Corbett, A.H. Kang, Animal collagenases: specificity of action, and structures of the substrate cleavage site, Biochem. Biophys. Res. Commun. 61 (1974) 605–612.